NASA TECHNICAL MEMORANDUM 108988

MODELING FATIGUE CRACK GROWTH IN CROSS PLY TITANIUM MATRIX COMPOSITES

J. G. Bakuckas, Jr. and W. S. Johnson

MAY 1993

This was presented to ASTM Fifth Symposium on Composite Materials: Fatigue and Fracture; Atlanta, Georgia; May 4-6, 1993

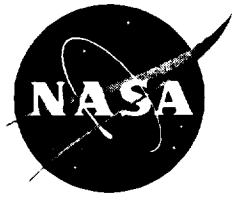

National Aeronautics and Space Administration

Langley Research Center
Hampton, Virginia 23681-0001

Abstract

In this study, the fatigue crack growth behavior of fiber bridging matrix cracks in cross-ply SCS-6/Ti-15-3 and SCS-6/Timetal-21S laminates containing center holes was investigated. Experimental observations revealed that matrix cracking was far more extensive and wide spread in the SCS-6/Ti-15-3 laminates compared to that in the SCS-6/Timetal-21S laminates. In addition, the fatigue life of the SCS-6/Ti-15-3 laminates was significantly longer than that of the SCS-6/Timetal-21S laminates. The matrix cracking observed in both material systems was analyzed using a fiber bridging (FB) model which was formulated using the boundary correction factors and weight functions for center hole specimen configurations. A frictional shear stress is assumed in the FB model and was used as a curve fitting parameter to model matrix crack growth data. The higher frictional shear stresses calculated in the SCS-6/Timetal-21S laminates resulted in lower stress intensity factors in the matrix and higher axial stresses in the fibers compared to those in the SCS-6/Ti-15-3 laminates at the same applied stress levels.

Nomenclature

a, a_o	Current crack length and unbridged initial crack length, mm
C, n	Paris crack growth coefficient constants
E_f, E_m	Fiber and matrix modulus, MPa
E_L	Composite longitudinal modulus, MPa
E_T	Composite transverse modulus, MPa
F_{app}	Boundary correction factor applied stress intensity factor
G_{bridge}	Weight function for bridging stress intensity factor
G_{LT}	Composite shear modulus, MPa
ΔK	Mode I stress intensity factor range, MPa$\sqrt{m}$
ΔK_{app}	Applied stress intensity factor range, MPa$\sqrt{m}$
K_P	Stress intensity factor for a concentrated force, P, applied to crack surface
ΔK_m	Discrete stress intensity factor range in matrix, MPa$\sqrt{m}$
ΔK_{tip}	Continuum stress intensity factor range in composite, MPa$\sqrt{m}$
ℓ	Slip length, m
max	Superscript referring to maximum applied load
min	Superscript referring to minimum applied load
P	Concentrated force applied on crack surface
Δp	Range in bridging pressure, MPa
r	Hole radius, m
r_f	Fiber radius, m
R	Stress ratio = S_{min}/S_{max}

ΔS	Applied stress range, MPa
v_f, v_m	Fiber and matrix volume fractions
$\tilde{x}$	Integration variable along crack from center, mm
$\Delta\delta_m$	Discrete crack opening displacement range in matrix, μm
$\Delta\delta_{tip}$	Continuum crack opening displacement range in composite, μm
τ	Interfacial frictional shear stress, MPa
ν_{LT}	Composite Poisson's ratio

Introduction

Titanium matrix composites (TMC) are being considered for high strength, low weight structural components for elevated temperature applications. However, before TMC can be confidently used for such applications, the complex state of damage that develops in these materials must be addressed. During fatigue loading of TMC, matrix cracks often develop and grow normal to 0° fibers without fibers breaking in the wake of these cracks [1-6]. As matrix cracks progress past the 0° fibers, fiber-matrix debonding occurs. This phenomena is called fiber bridging and it has a profound effect on the crack-tip stress intensity factor governing matrix crack growth behavior. In spite of fibers remaining intact, matrix cracking and fiber-matrix debonding significantly reduce the composite longitudinal modulus and post-fatigue residual strength [4,5]. Thus, the growth of fiber bridging matrix cracks is of particular concern and is the main focus of this study.

Much effort has been directed towards modeling the crack growth behavior of fiber bridging matrix cracks [6-9]. Several of the pioneering fiber bridging (FB) models [7-9] were reviewed and applied to study matrix crack growth behavior in center notched, unidirectional TMC [6]. In these FB models, continuum fracture mechanics and micromechanics analyses are combined to derive stress intensity factor solutions of fiber bridging matrix cracks. The unknown constant frictional shear stress, τ, assumed in these models was used as a curve fitting parameter to available data in [6]. In general, as τ increased, the calculated matrix stress intensity factor, crack opening displacement, and slip length all decreased. There were large differences in the values of τ used to correlate the data. The value of τ depended on the crack length, applied stress level, and distance from the first intact fiber and, thus, is not a material property. Currently, the FB models

lack true predictive capabilities due to the dependency of τ on so many factors. The FB models may provide a framework for future crack growth prediction methodologies. The study in [6] revealed that the FB models provided an efficient and relatively simple engineering approach to conduct parametric analysis and helped in the interpretation of the experimental results.

The primary emphasis of this research was to experimentally study and analytically model the fatigue crack growth behavior of fiber bridging matrix cracks in cross-ply SCS-6/Ti-15-3 laminates and SCS-6/Timetal-21S (formally referred to as SCS-6/β21S) laminates containing center holes. Experimentally, constant amplitude, tension-tension (R = 0.1) fatigue tests were conducted under load control mode at a frequency of 10 Hz. Matrix crack initiation and growth were monitored using a high magnification closed circuit television (CCTV) system, a long focal length microscopic system with image acquisition capabilities, surface and edge replicas, optical microscopy, and scanning electron microscopy (SEM). Analytically, the matrix cracking observed in both material systems was modeled using a fiber bridging (FB) model which was formulated using the boundary correction factor and weight function for symmetric cracks emanating from a hole. The frictional shear stress term, τ, in this model was used as a curve fitting parameter to matrix crack growth data. Experimental results were interpreted from the analysis made using the FB model.

Materials and Test Procedure

Two TMC systems having cross-ply lay-ups containing center holes were studied in this research, namely, SCS-6/Ti-15-3 laminates and SCS-6/Timetal-21S laminates. Both TMC systems were fabricated by Textron by hot isostatic pressing (HIPing) titanium foils between unidirectional tapes of silicon-carbide (SCS-6) fibers having a diameter of 0.14 mm. The fibers were held in place with molybdenum and titanium-niobium cross weave wires in the SCS-6/Ti-15-3 and SCS-6/Timetal-21S laminates, respectively. The lay-ups studied were $[0/90]_s$, and $[0/90]_{2s}$ with a range of fiber volume fractions v_f of 0.34 to 0.38. In the SCS-6/Ti-15-3 laminates and the SCS-6/Timetal-21S laminates, the composition of the titanium matrices were Ti-15V-3Cr-3Al-3Sn and Ti-15Mo-3Al-2.7Nb-0.2Si, respectively.

Specimens were cut using a diamond wheel saw into straight-sided coupons with the 0° fibers in the loading direction. Each specimen was 152.4-mm long and 19.1-mm wide. Center holes having diameter-to-width ratios (d/W) of 0.32 and 0.35 were drilled ultrasonically. The SCS-6/Ti-15-3 specimens were tested in the as-received condition while the SCS-6/Timetal-21S specimens were heat treated at a temperature of 620°C for 8 hours in vacuum and then oven cooled prior to testing. To make optical observations and replicas, the surface of each specimen was polished to obtain a flat and lustrous finish. Aluminum end tabs were bonded on all specimens in order to prevent grip failure.

Constant amplitude, tension-tension fatigue tests were conducted under load control with R = 0.1 at a frequency of 10 Hz using a closed-loop servo-hydraulic test machine equipped with hydraulic grips. Matrix crack initiation and progression were monitored and recorded in real time using a CCTV having magnification capabilities up to 325X and a long focal length microscopic system with image acquisition capabilities. Testing was periodically interrupted when significant increments in crack extension were observed in order to take surface replicas and to examine the specimens surface using the SEM and an optical microscope.

Analysis - Fiber Bridging Model

The fiber bridging phenomena that often occurs during fatigue loading of TMC was modeled using a fiber bridging (FB) model similar to those outlined in [7-9]. As illustrated in Figure 1, it is assumed in this model that fiber-matrix debonding takes place as a matrix crack progresses past the fibers. The intact fibers in the wake of the matrix crack are idealized as a crack bridging pressure, Δp. An unknown constant frictional shear stress, τ, is assumed to act along the debond length of the bridging fibers. A continuum fracture mechanics analysis and a micromechanical analysis are combined to obtain stress intensity factor solutions for fiber bridging matrix cracks of arbitrary size. In this study, the boundary correction factors and weight functions developed in [10,11] were implemented into a FB model in order to account for cracks developing in a center hole specimen configuration. The derivation of the governing equation is outlined in the subsequent sections.

Analysis Procedure

Conventional fracture mechanics characterization of Mode I fatigue crack growth behavior is accomplished through the relation between the crack growth rate and the stress intensity factor range. In this study the crack growth behavior is modeled according to the power law function introduced by Paris et al. [12]:

$$\frac{da}{dN} = C(\Delta K_m)^n \tag{1}$$

where C and n are material constants for the matrix material. The term ΔK_m is the Mode I stress intensity factor range in the matrix and is determined using a FB model which combines a continuum fracture mechanics and a discrete micromechanics analyses. In the continuum fracture mechanics analysis, the stress intensity factor in the composite, ΔK_{tip}, and the crack opening displacement in the composite, $\Delta\delta_{tip}$, are given in terms of the unknown bridging pressure, Δp. In the micromechanics analysis, the crack opening displacement in the matrix, $\Delta\delta_m$, is related to Δp through the composite microstructural parameters which includes the frictional shear stress in the debonding region, τ.

Several continuum-discrete relations are used to relate $\Delta\delta_{tip}$ with $\Delta\delta_m$, and ΔK_{tip} with ΔK_m (see, for example, [6]) which ultimately yields a single equation in terms of the unknown Δp. The continuum-discrete relations in [9] ($\Delta\delta_{tip} = \Delta\delta_m$, and $\Delta K_{tip} = \Delta K_m$), produced the most accurate correlations with experimental data with the least variation in frictional shear stress for unidirectional TMC containing center notches [6] and were thus used in this study.

Assuming a value of τ, the bridging pressure, Δp, can be solved. Knowing Δp, the stress intensity factor range in the matrix, ΔK_m, can be evaluated and then used in Equation (1) to model the crack growth behavior of fiber bridging matrix cracks. A brief description of the continuum fracture mechanics analysis, the discrete micromechanics analysis and the governing equation is provided in the following sections.

Continuum Fracture Mechanics Analysis

The continuum fracture mechanics analysis in the FB models provides solutions to the composite stress intensity factor (ΔK_{tip}) and the composite crack opening displacement ($\Delta\delta_{tip}$) in terms of the unknown bridging pressure (Δp). Assuming $\Delta K_{tip} = \Delta K_m$:

$$\Delta K_m = \Delta K_{app} - 2\int_{a_o}^{a} G_{bridge}(x,a,r,W)\Delta p(x)dx \qquad (2)$$

where a_o is the initial unbridged crack length (hole radius, r) and G_{bridge} is the weight function for the bridging stress intensity factor range defined as:

$$G_{bridge} = \frac{dK_P}{dP} \qquad (3)$$

In Equation (3), K_P is the stress intensity factor due to a pair of concentrated forces, P, applied on the crack surface at a distance x from the origin, as shown in Figure 2. The term ΔK_{app} in Equation (2) is the applied stress intensity factor range given by:

$$\Delta K_{app} = \Delta S \sqrt{\pi a}\, F_{app} \qquad (4)$$

where ΔS is the applied far-field stress, F_{app} is the applied stress boundary correction factor. A compendium of boundary correction factors and weight functions, F_{app} and G_{bridge}, is provided in [13] for a variety of cracked specimen configurations. For the case of symmetric cracks emanating from a center hole, expressions for F_{app} and G_{bridge} were derived in [10,11] and are provided in the Appendix for the sake of completeness. It should be pointed out that the boundary correction factors and the weight functions in [10,11,13] were derived for isotropic materials and it was assumed that these terms can be applied to the orthotropic materials studied in this research.

The opening displacements of the crack surfaces, $\Delta\delta_{tip}$, is determined using Castigliano's Theorem as outlined in [13]. Assuming $\Delta\delta_{tip} = \Delta\delta_m$:

$$\Delta\delta_m = \frac{2}{E'} \int_x^a \left\{ \Delta K_m(x,\tilde{a},r,W) \frac{dK_P}{dP}(x,\tilde{a},r,W) \right\} d\tilde{a} \tag{5}$$

where E' for an orthotropic material is [14]:

$$\frac{1}{E'} = \frac{1}{2E_L} \left(\sqrt{2\left\{ \sqrt{\frac{E_L}{E_T}} - \nu_{LT} \right\} + \frac{E_L}{G_{LT}}} \right) \tag{6}$$

The terms in this equation are the laminate elastic properties as defined in the nomenclature.

Discrete Micromechanics Analysis

In the micromechanics analysis, the matrix crack opening displacement, $\Delta\delta_m$, is related to the unknown bridging pressure, Δp, through the composite microstructural parameters as outlined in detail in [6]. The force equilibrium of a single fiber in the wake of the matrix crack results in:

$$\Delta\delta_m = \lambda \Delta p^2 \tag{7}$$

where:

$$\lambda = \frac{r_f E_m \nu_m}{4\tau \nu_f^2 E_f (E_f \nu_f + E_m \nu_m)} \tag{8}$$

The terms in this equation are the composite microstructural parameters as defined in the nomenclature. The frictional shear stress, τ, in Equation (8) is an ambiguous quantity that is difficult to directly measure. In this study, τ was used as a fitting parameter to crack growth data.

Governing Equation

Substituting Equation (7) into (5), the governing equation is obtained in the form of a nonlinear double integral equation in terms of unknown bridging pressure, Δp:

$$\Delta p^2 = \frac{2}{\lambda E'} \int_x^a \left\{ \Delta K_m(x,\tilde{a},r,W) \frac{dK_P}{dP}(x,\tilde{a},r,W) \right\} d\tilde{a} \tag{9}$$

Using a Newton-Raphson iterative process and a Simpson type algorithm for numerical integration, the governing equation is solved. Once the bridging pressure is known, the matrix

stress intensity factor range, ΔK_m, can obtained using Equation (2). Knowing ΔK_m, standard damage tolerance procedures can be used to model the crack growth behavior. In this study, Equation (1) was numerically integrated using a Simpsons type algorithm to generate the matrix crack length as a function of number of cycles.

Application of FB Model to Cross Ply Laminates

In order to apply the FB model to cross-ply laminates, it was assumed that matrix cracking was controlled primarily by the fibers in the 0° plies and was not affected by the fibers in the 90° plies. Thus, in the micromechanics analysis, the 90° plies were modeled as matrix material by using one half of the laminates fiber volume fraction, v_f, in Equation (8). It was also assumed that the cracking in the 90° plies was a local effect and did not influence the far-field properties. Thus, in the continuum fracture mechanics analysis, the actual fiber volume fraction was used in calculating the laminate properties for the orthotropic correction factor, E', in Equation (6).

Results and Discussion

In this section, experimental results of the matrix crack growth in center hole cross-ply TMC, namely, SCS-6/Timetal-21S laminates and SCS-6/Ti-15-3 laminates are discussed first. The experimental data generated in the current study for the SCS-6/Timetal-21S laminates is presented along with the data reported in [5] for the SCS-6/Ti-15-3 laminates. Then results from the analytical modeling of the observed crack growth behavior are outlined in which the frictional shear stress in the FB model was used as a curve fitting parameter to matrix crack growth data. Finally, experimental results were interpreted from the analysis using the FB model.

Experimental Results

Damage initiation and progression was monitored and recorded during fatigue loading in cross-ply TMC containing center holes. Fatigue damage in SCS-6/Timetal-21S laminates consisted primarily of Mode I matrix cracks as shown for example in Figure 3. As illustrated in

this figure for one side of the center hole in the specimen, two matrix cracks initiated and progressed in a specimen subjected to S_{max} = 150 MPa. Similar cracking occurred on the other side of the hole. After 200,000 cycles, the rate of growth of the matrix cracks corresponded to a stress intensity factor range near the threshold value for the neat matrix material subjected to R = 0.1, $\Delta K_{th} \approx 5.5$ MPa$\sqrt{m}$ (unpublished data reported by R. John and N. E. Ashbaugh, University of Dayton Research Institute, 1992).

Fatigue damage was far more extensive in the SCS-6/Ti-15-3 specimens where multiple Mode I matrix cracks developed from the center hole as shown for example in Figure 4 [5]. This figure shows schematics taken directly from the CCTV monitor of matrix crack development on one side of the hole of a specimen during fatigue loading at S_{max} = 200 MPa. During this test, matrix cracking initiated and progressed from the edge of the center hole as shown in Figure 4(a) (cracks 1 and 2). As these matrix cracks continued to grow, secondary cracks formed in net section regions away from the edge of the center hole, Figure 4(b) (cracks 4 and 7). In addition, matrix cracks (cracks 3, 5 and 6) developed in regions above and below the original matrix cracks (cracks 1 and 2). Matrix cracks continued to propagate and link-up until cracking reached a saturated state, Figure 4(c). Saturation was assumed when no additional matrix cracks initiated and when existing cracks no longer grew. For this specimen, saturation occurred after 150,000 cycles. As shown in the figure, the matrix cracks have a uniform spacing a short distance (approximately 1 mm) away from the center hole. Similar cracking patterns (multiple matrix cracks) were observed in [1,2] for $[0/90]_{2s}$ SCS-6/Ti-15-3 laminates containing center holes.

In spite of the observed matrix cracking on the surface as shown for example in Figures 3 and 4, the underlying 0° fibers were intact. In selected specimens, the outer layer of matrix material was removed through an acid etching procedure to reveal the 0° fibers. Observations made using the SEM revealed no fiber breaks in the SCS-6/Timetal-21S specimens tested in this study as well as the SCS-6/Ti-15-3 laminates tested in [5].

The matrix crack length as a function of the number of cycles was obtained at several applied stress levels and is shown in Figures 5 and 6 for the SCS-6/Timetal-21S laminates and the

SCS-6/Ti-15-3 laminates, respectively. In these figures, the average length of the cracks progressing from the center hole is shown. It should be pointed out that in all cases cracks grew on both sides of the hole at similar rates. For the SCS-6/Ti-15-3 laminates, the cycle number at which the initiation of matrix cracks other than the ones progressing from the center hole are noted (data points designated by filled symbols), Figure 6. Only the matrix crack growth data designated by open symbols in Figure 6 was subsequently evaluated. Under a constant applied stress range, the matrix crack extension decreased as the number of cycles increased in both material systems due primarily to the bridging fibers, Figures 5 and 6. Also shown in these figures, the extent of matrix cracking increased as the applied stress level increased.

The rate of matrix cracking as a function of crack length for several applied stress levels is shown in Figures 7 and 8 for the SCS-6/Timetal-21S laminates and SCS-6/Ti-15-3 laminates, respectively. In both cases, the rate of matrix cracking decreased as the crack length increased and increased as the applied stress increased. In general, by comparing the results from Figures 7 and 8, the rate and extent of matrix cracking in the SCS-6/Ti-15-3 laminates was greater than that in the SCS-6/Timetal-21S laminates.

Characterization of the in-situ matrix fatigue crack growth behavior using the neat matrix material properties was attempted using the applied stress intensity factor range, Equation (4). Using standard data reduction procedures (ASTM Standard E 647), the crack growth rate as a function of the applied stress intensity factor range (ΔK_{app}) for the neat matrix materials (at R = 0.1) and for the TMC is shown in Figures 9 and 10 for the SCS-6/Timetal-21S laminates and the SCS-6/Ti-15-3 laminates, respectively. As shown in these figures, ΔK_{app} in the composite significantly over estimates the actual stress intensity driving the matrix cracks. In addition, the crack growth rate tends to decrease as the applied stress intensity increases due to the bridging fibers in both materials. Thus, the applied stress intensity factor range is inappropriate to model the growth of fiber bridging matrix cracks.

The applied nominal stress as a function of the number of cycles (S-N curve) is shown in Figure 11 for the SCS-6/Timetal-21S laminates and SCS-6/Ti-15-3 laminates. In this figure, the

solid symbols are data from specimens that fractured, while the open symbols are data from specimens that did not fail. In general, the results from this figure reveals that the fatigue lives of the SCS-6/Timetal-21S laminates are shorter compared to SCS-6/Ti-15-3 laminates subjected to similar applied stresses.

Analytical Results

Using the previously mentioned FB model, the stress intensity factor range in the matrix, ΔK_m, was calculated by curve fitting the frictional shear stress, τ, to the matrix crack growth data for both the Timetal-21S and Ti-15-3 titanium alloys. By adjusting the constant frictional shear stress, the in-situ matrix crack growth data were collapsed onto that of the neat matrix material for both material systems, Figures 12 and 13. Compared to Figures 9 and 10, the data is shifted to a lower stress intensity factor range and is rotated towards a positive slope due to the fiber bridging as modeled by the bridging pressure term in Equation (2). Using the FB model, an appropriate expression for ΔK_m was obtained for fiber bridging matrix cracks.

By integrating Equation (1) using the calculated ΔK_m from Figures 12 and 13, the crack length as a function of the number of cycles was determined and is shown in Figures 14 and 15 for the SCS-6/Timetal-21S laminates and the SCS-6/Ti-15-3 laminates, respectively. As shown in these figures, a good agreement was obtained between the observations (open symbols) and calculations (filled symbols) indicating the good fit for τ and the appropriateness of Equation (1) in describing the fatigue crack growth behavior.

Using the frictional shear stress values fitted to the matrix crack growth data, the calculated stress in the first intact fiber as a function of the number of cycles for several applied stress levels is shown in Figures 16 and 17 for the SCS-6/Timetal-21S laminates and the SCS-6/Ti-15-3 laminates, respectively. As shown in these figures, the fiber stress increased as both the number of cycles and the applied stress level increased. The fiber stresses in the SCS-6/Timetal-21S laminates were higher than those calculated for the SCS-6/Ti-15-3 laminates. Apparently in the SCS-6/Timetal-21S laminates, the stresses in the fibers reached a critical value sufficiently high to

fracture the fibers at a lower number of fatigue cycles resulting in the lower fatigue life compared to the SCS-6/Ti-15-3 laminates.

The values of the frictional shear stress used to fit the crack growth data for the SCS-6/Timetal-21S laminates were higher than those for the SCS-6/Ti-15-3, Figures 12 and 13. This result would suggest the following three hypotheses: (1) the radial thermal residual stresses acting across the debonded surfaces causing the matrix to "choke" the fibers were higher in the SCS-6/Timetal-21S; (2) the coefficient of friction due to the roughness of the debonded surfaces was higher in the SCS-6/Timetal-21S laminates; and (3) the length of the debond was less in the SCS-6/Timetal-21S. All three hypotheses would cause an increase in the frictional shear stress acting along the debonded fiber-matrix interface. The effect of the frictional shear stress on the stress intensity factor range in the matrix and the stress in the first intact fiber is shown in Figure 18 for a center notched unidirectional SCS-6/Ti-15-3 specimen tested in [6]. As shown in this figure, as τ increases, the fiber stress increases while ΔK_m decreases. This trend (not shown here) was also observed for the materials investigated in this research. Thus, the fibers would more likely fracture in the SCS-6/Timetal-21S laminates whereas, matrix cracks would more likely propagate in the SCS-6/Ti-15-3 laminates which is in agreement with experimental observations.

Concluding Remarks

The primary emphasis of this research was to model the fatigue crack growth behavior of fiber bridging matrix cracks in cross-ply SCS-6/Ti-15-3 and SCS-6/Timetal-21S laminates containing center holes. Experimental results revealed that matrix cracking was more extensive and wide spread in the SCS-6/Ti-15-3 laminates compared with the SCS-6/Timetal-21S laminates. In addition, the fatigue life of the SCS-6/Ti-15-3 laminates was significantly longer than that of the SCS-6/Timetal-21S laminates. The standard practice of characterizing fatigue crack growth using the applied stress intensity factor range was not suitable. Thus, a fiber bridging (FB) model which was formulated using the boundary correction factor and weight function for symmetric cracks emanating from a hole was used to model the observed matrix cracking. The FB model combines continuum fracture mechanics and micromechanics analyses to derive stress intensity factor

solutions of matrix cracks bridged by fibers in a unidirectional composite. In order to apply the FB model to cross-ply laminates, it was assumed that matrix cracking was a local phenomena controlled primarily by the fibers in the 0° plies and was not affected by the fibers in the 90° plies. Thus, in the micromechanics analysis, the 90° plies were modeled as matrix material by using one half of the laminates fiber volume fraction; while in the continuum fracture mechanics analysis, the actual fiber volume fraction was used.

The frictional shear stress assumed in the FB model was used as a curve fitting parameter to matrix crack growth data. The frictional shear stress values required to fit the crack growth data for the SCS-6/Timetal-21S laminates were higher than those for the SCS-6/Ti-15-3 laminates. Consequently, lower stress intensity factors in the matrix and higher stresses in the fibers were predicted in the SCS-6/Timetal-21S laminates compared with the SCS-6/Ti-15-3 laminates at the same applied stress levels. Thus, fibers were more prone to fracture in the SCS-6/Timetal-21S laminates whereas, more extensive matrix cracking was likely in the SCS-6/Ti-15-3 laminates.

Acknowledgements

The first author gratefully acknowledges the support extended by the National Research Council, Washington, D.C., through their Associateship Program. The crack growth data for the neat Timetal-21S matrix material shown in Figures 9 and 12 was obtained from R. John and N. E. Ashbaugh, University of Dayton Research Institute, 1992.

References

[1] Hillberry, B. M. and Johnson, W. S., "Matrix Fatigue Crack Development in a Notched Continuous Fiber SCS-6/Ti-15-3 Composite," *Symposium on Microcracking Induced Damage in Composites,* ASME Winter Annual Meeting, 1990, pp. 121-127.

[2] Naik, R. A., and Johnson, W. S., "Observations of Fatigue Crack Initiation and Damage Growth in Notched Titanium Matrix Composites," *Third Symposium on Composite Materials: Fatigue and Fracture, ASTM STP 1110,* T. K. O'Brien, Ed.,1991, pp. 753-771.

[3] Harmon, D. M., and Saff, C. R.,"Damage Initiation and Growth in Fiber Reinforced Metal Matrix Composites," *Metal Matrix Composites: Testing, Analysis and Failure, ASTM STP 1032,* W, S. Johnson, Ed., ASTM, 1989, pp. 237-250.

[4] Johnson, W. S., "Fatigue of Continuous Fiber Reinforced Titanium Metal Matrix Composites," *Mechanical Fatigue of Advanced Materials,* Ritchie, Cox and Dauskardt, Eds., MCEP Publishers, 1991, pp.357-378.

[5] Bakuckas, J. G. Jr., Johnson, W. S., and Bigelow, C. A.,"Fatigue Damage in Cross-Ply Titanium Metal Matrix Composites Containing Center Holes, *NASA TM 104197,* 1992.

[6] Bakuckas, J. G., Jr., and Johnson, W. S.,"Application of Fiber Bridging Models to Fatigue Crack Growth in Unidirectional Titanium Metal Matrix Composites," *NASA Technical Memorandum 107588,* 1992.

[7] Marshall, D. B., Cox, B. N., and Evans, A. G., "The Mechanics of Matrix Cracking in Brittle-Matrix Fiber Composites," *Acta Metall.,* Vol. 33, No. 11, 1985, pp. 2013-2021.

[8] McCartney, L. N., "Mechanics of Matrix Cracking in Brittle-Matrix Fibre-Reinforced Composites," *Proc. R. Soc. Lond.,* A 409, pp. 329-350, 1987.

[9] McMeeking, R. M., and Evans, A. G., "Matrix Fatigue Cracking in Fiber Composites," *Mechanics of Materials,* Vol. 9, 1990, pp. 217-227.

[10] Newman, J. C., Jr., "A Nonlinear Fracture Mechanics Approach to the Growth of Small Cracks," *Behavior of Short Cracks in Airframe Components.,* AGARD Conference Proceedings No. 328, 1982, pp. 6.1 - 6.26.

[11] Newman, J. C., Jr., "An Improved Method of Collocation for the Stress Analysis of Cracked Plates with Various Shaped Boundaries," *NASA Technical Note D-6376,* 1971.

[12] Paris, P. C., Gomez M. P., and Anderson, W. E., "A Rational Analytic Theory of Fatigue," *The Trend in Engineering,* Vol. 13, pp. 9-14, 1961.

[13] Tada, H., Paris, P. C., and Irwin, G. R., *The Stress Analysis of Cracks Handbook,* Del Research Corporation, St. Louis, MO, 63105, 1985.

[14] Lekhnitskii, S. G., *Theory of Elasticity of an Anisotropic Body,* Holden-Day, San Francisco, 1963.

[15] Lenning, G. A, Hall, J. A., Rosenblum, M. E., and Trepel, W. B., "Cold Formable Titanium Sheet," *AFWAL-TR-82-4174,* December 1982.

Appendix - Boundary Correction Factor and Weight Function

For two symmetric cracks progressing from a center hole of radius r in an isotropic material, the applied stress boundary correction factor is [10]:

$$F_{app} = F_1 F_2 \tag{A1}$$

where:

$$F_1 = \left\{1 + 0.358\frac{r}{a} + 1.425\left(\frac{r}{a}\right)^2 - 1.578\left(\frac{r}{a}\right)^3 + 2.156\left(\frac{r}{a}\right)^4 \right\}\sqrt{1 - \frac{r}{a}} \tag{A2}$$

and:

$$F_2 = \sqrt{\sec\frac{\pi r}{W}\sec\frac{\pi a}{W}} \tag{A3}$$

The weight function, G_{bridge}, for two symmetric concentrated forces, P, applied to the cracks surface in a center hole specimen configuration, Figure 2 [10]:

$$G_{bridge} = \frac{dK_P}{dP} = \frac{dK_P^{cn}}{dP} F_h \tag{A4}$$

In this equation, $\frac{dK_P^{cn}}{dP}$ is the normalized stress intensity factor for a center notched specimen configuration subjected to a pair of forces, P, on the crack surface and F_h is the correction factor to account for a center hole boundary. The normalized stress intensity for a center notched specimen is given by [13]:

$$\frac{dK_P^{cn}}{dP} = \left\{1 + 0.297\sqrt{1 - \left(\frac{x}{a}\right)^2}\,(1 - \cos\frac{\pi a}{W})\right\} F_{III} \tag{A5}$$

where:

$$F_{III} = \sqrt{\frac{1}{W}\tan\frac{\pi a}{W}}\,\frac{\cos\frac{\pi x}{W}}{\sqrt{\cos\left(\frac{\pi x}{W}\right)^2 - \cos\left(\frac{\pi a}{W}\right)^2}} \tag{A6}$$

The correction factor to account for the center hole is given by [10]:

$$F_h = 1 + A_1\left\{\frac{a - x}{a - r}\right\} + A_2\left\{\frac{a - x}{a - r}\right\}^2 \tag{A7}$$

where:

$$A_1 = -0.020\left(\frac{r}{a}\right)^2 + 0.558\left(\frac{r}{a}\right)^4 \tag{A8}$$

$$A_2 = 0.221\left(\frac{r}{a}\right)^2 + 0.046\left(\frac{r}{a}\right)^4 \tag{A9}$$

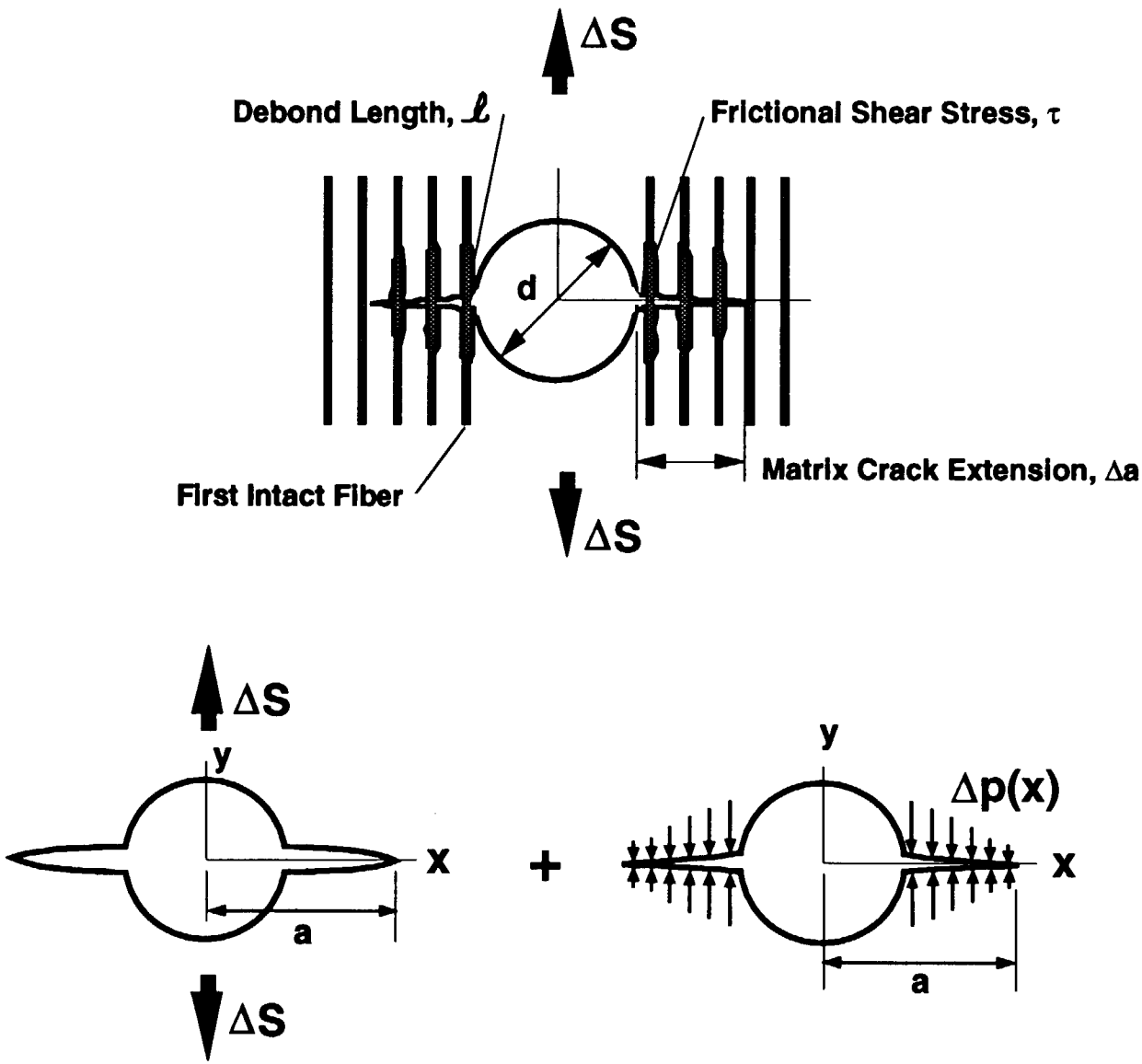

Figure 1. Continuum fracture mechanics approximation of matrix crack growth process. Fibers bridging crack are idealized as a closure pressure. Governing equation is formulated by superposition of a crack subjected to a far-field applied stress and a crack subjected to a closure pressure.

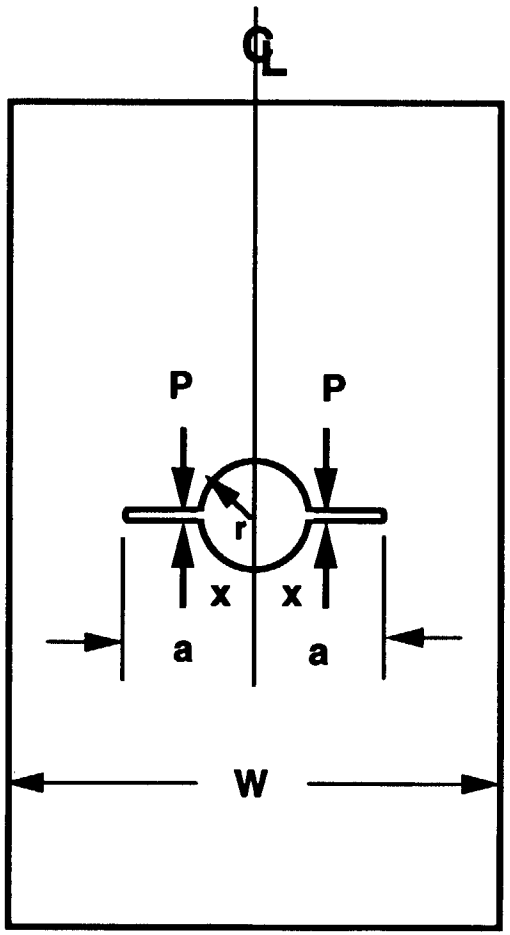

Figure 2. Center hole specimen configuration with two symmetric cracks. A concentrated force, P, is applied on the crack surface a distance x from the origin.

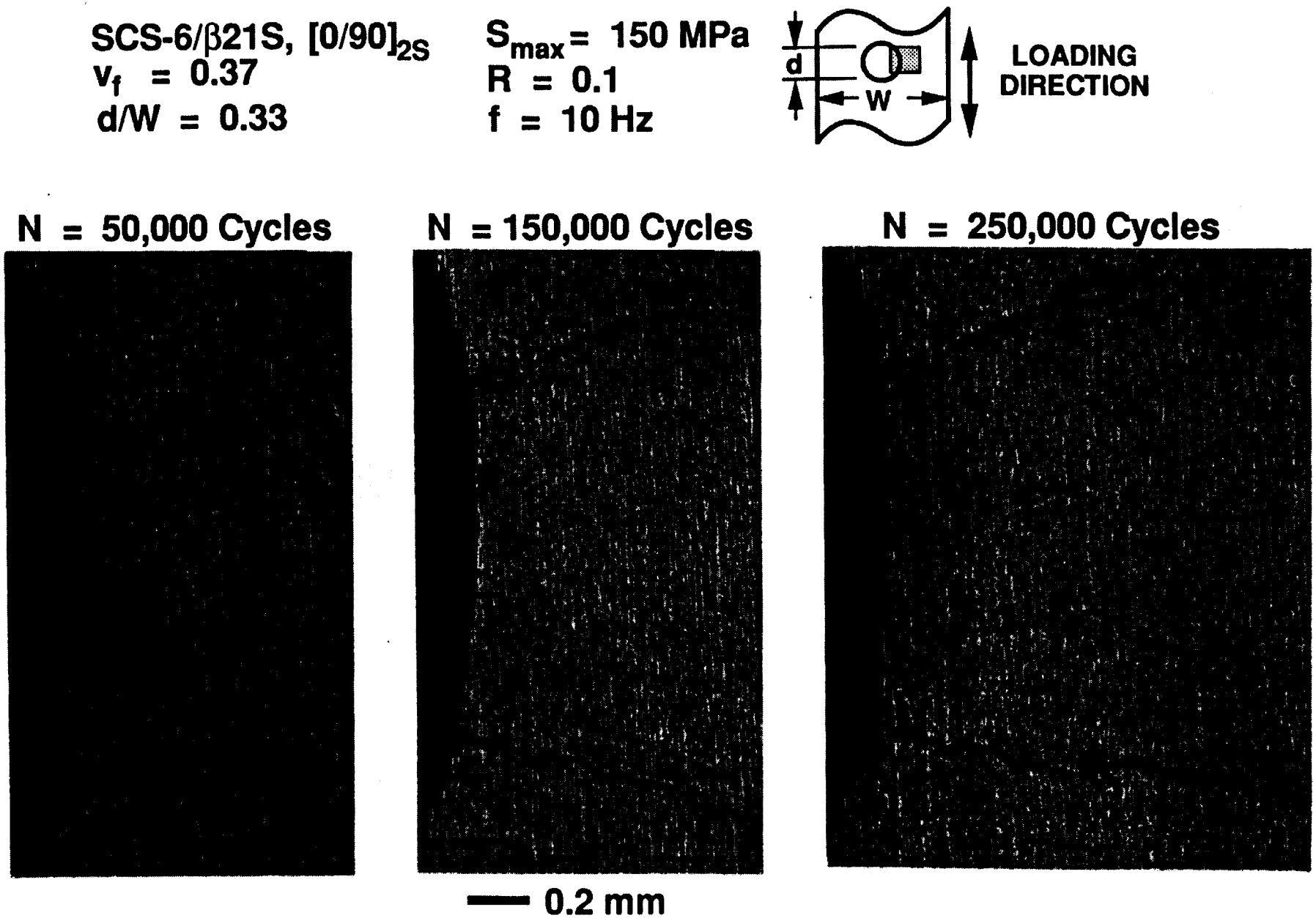

Figure 3. Development of matrix cracks in a $[0/90]_{2s}$ SCS-6/Timetal-21S laminate containing a center hole.

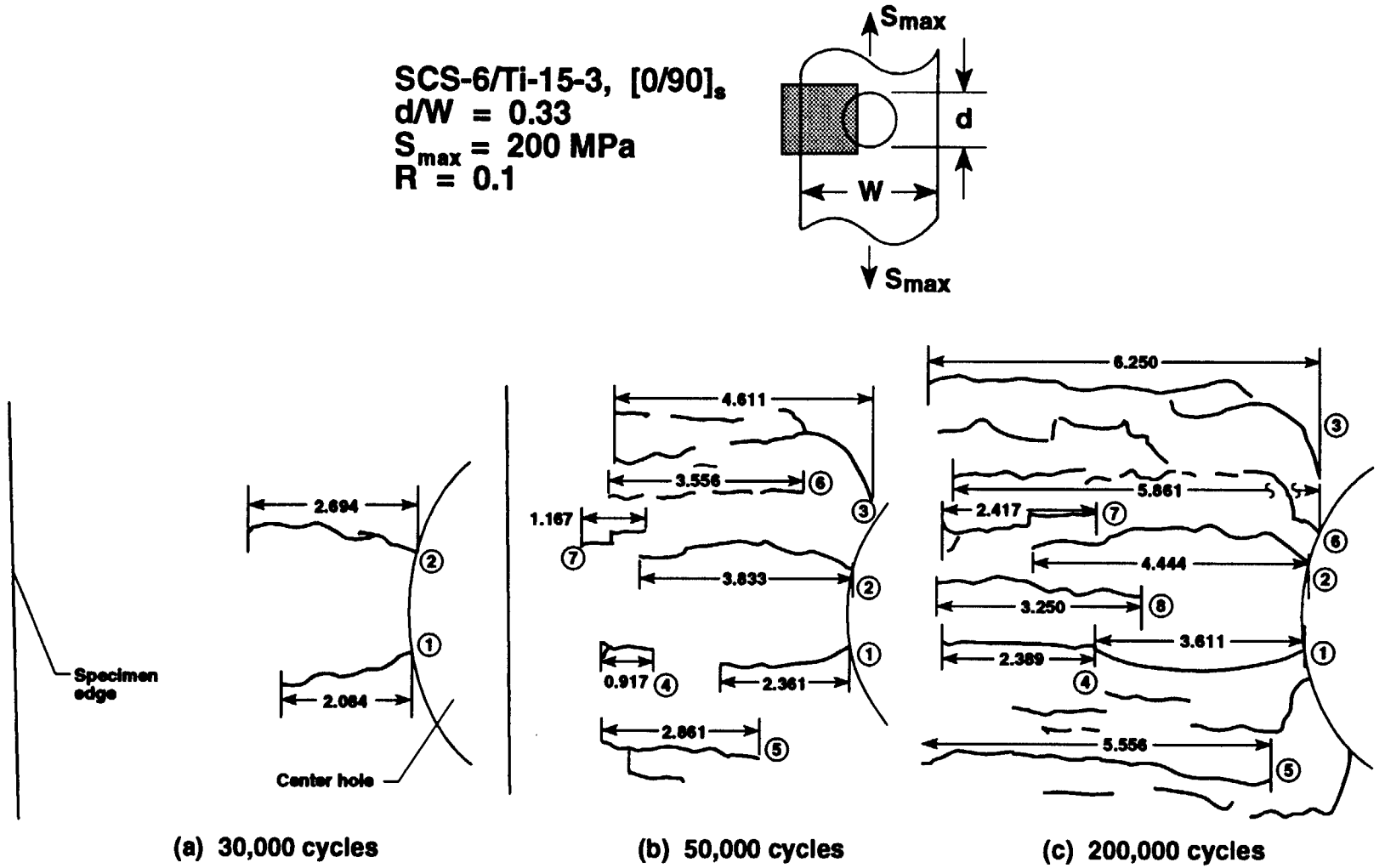

Figure 4. Development of matrix cracks in a $[0/90]_s$ SCS-6/Ti-15-3 laminate containing a center hole, v = 0.355; (a) initiation of cracks; (b) development of secondary cracks; (c) saturation of matrix cracks. Schematics are not to scale [5].

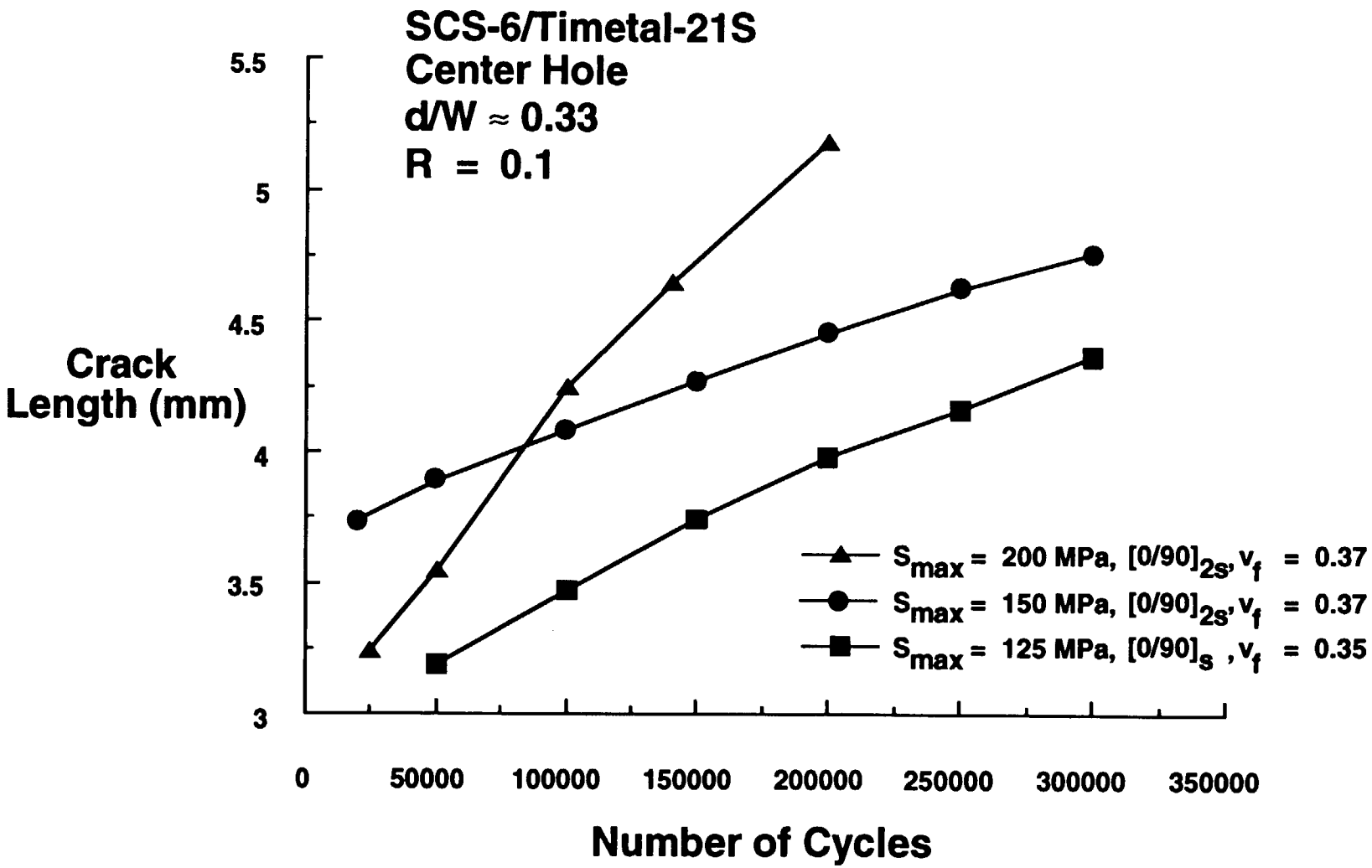

Figure 5. Total average crack length as a function of number of cycles in cross ply, SCS-6/Timetal-21S laminates containing holes.

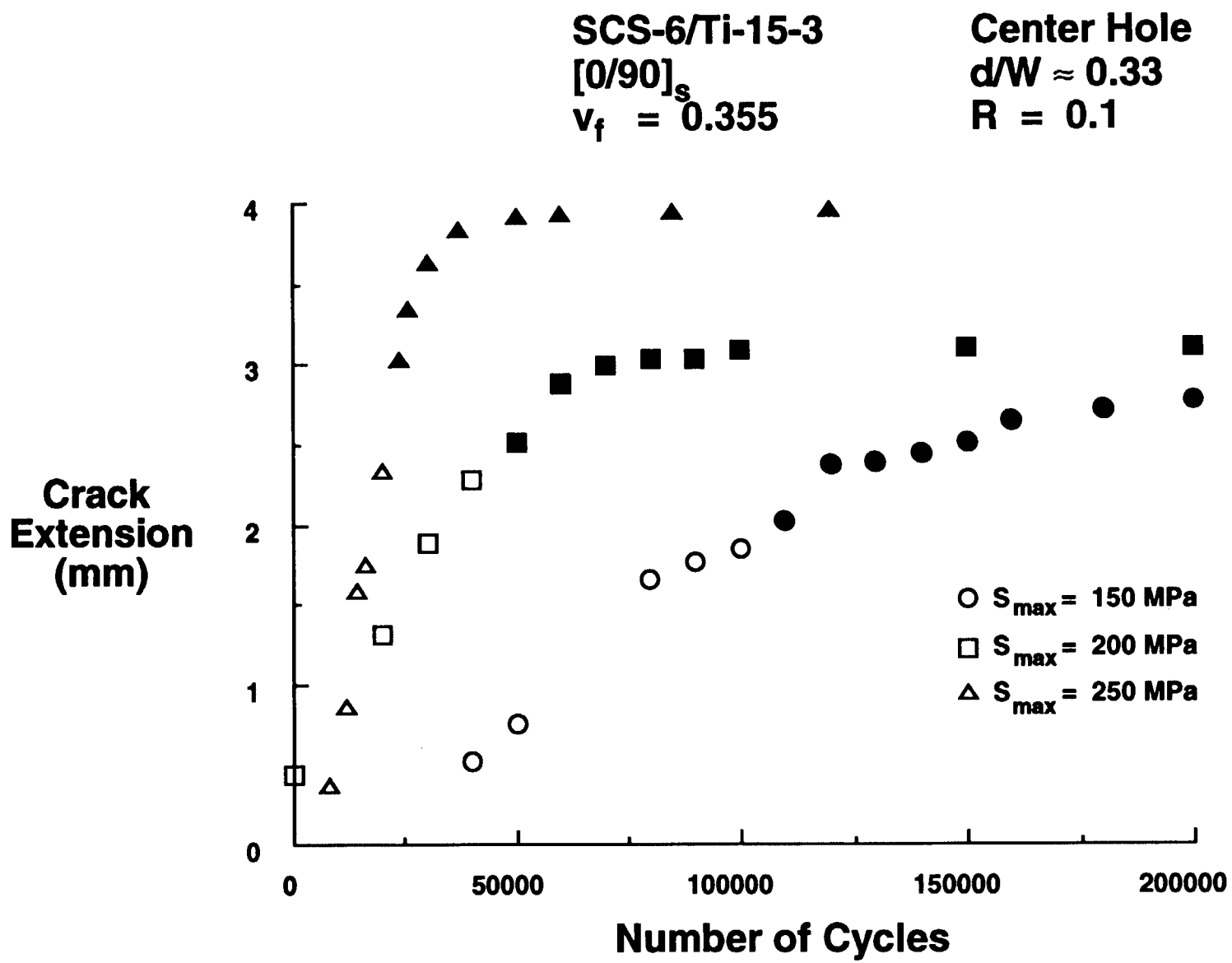

Figure 6. Average crack extension of matrix cracks progressing from center hole. As the number of cycles increases, the rate of crack growth decreases due to bridging fibers.

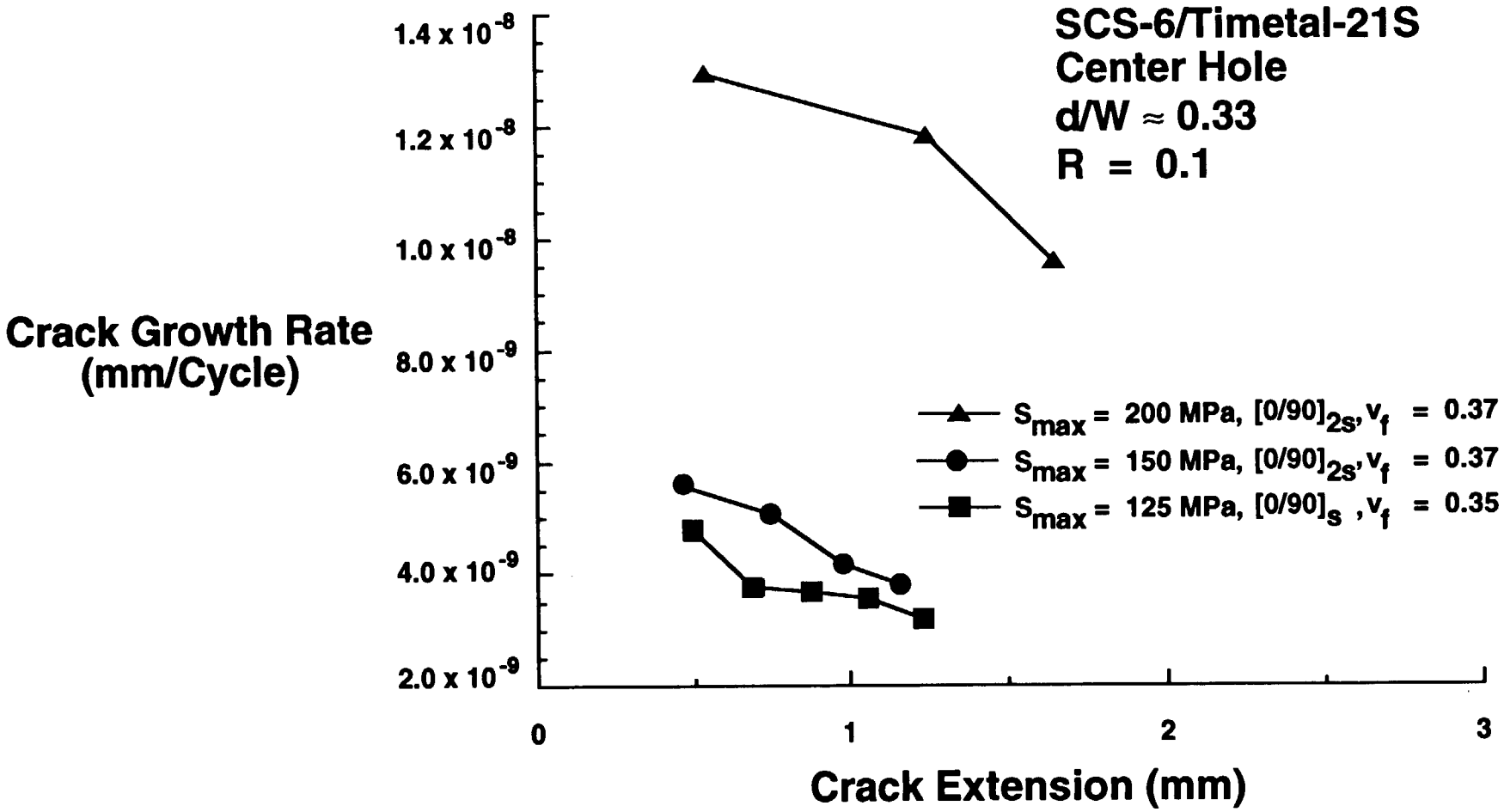

Figure 7. Crack growth rate as a function of number of cycles in cross ply, SCS-6/Timetal-21S laminates containing holes.

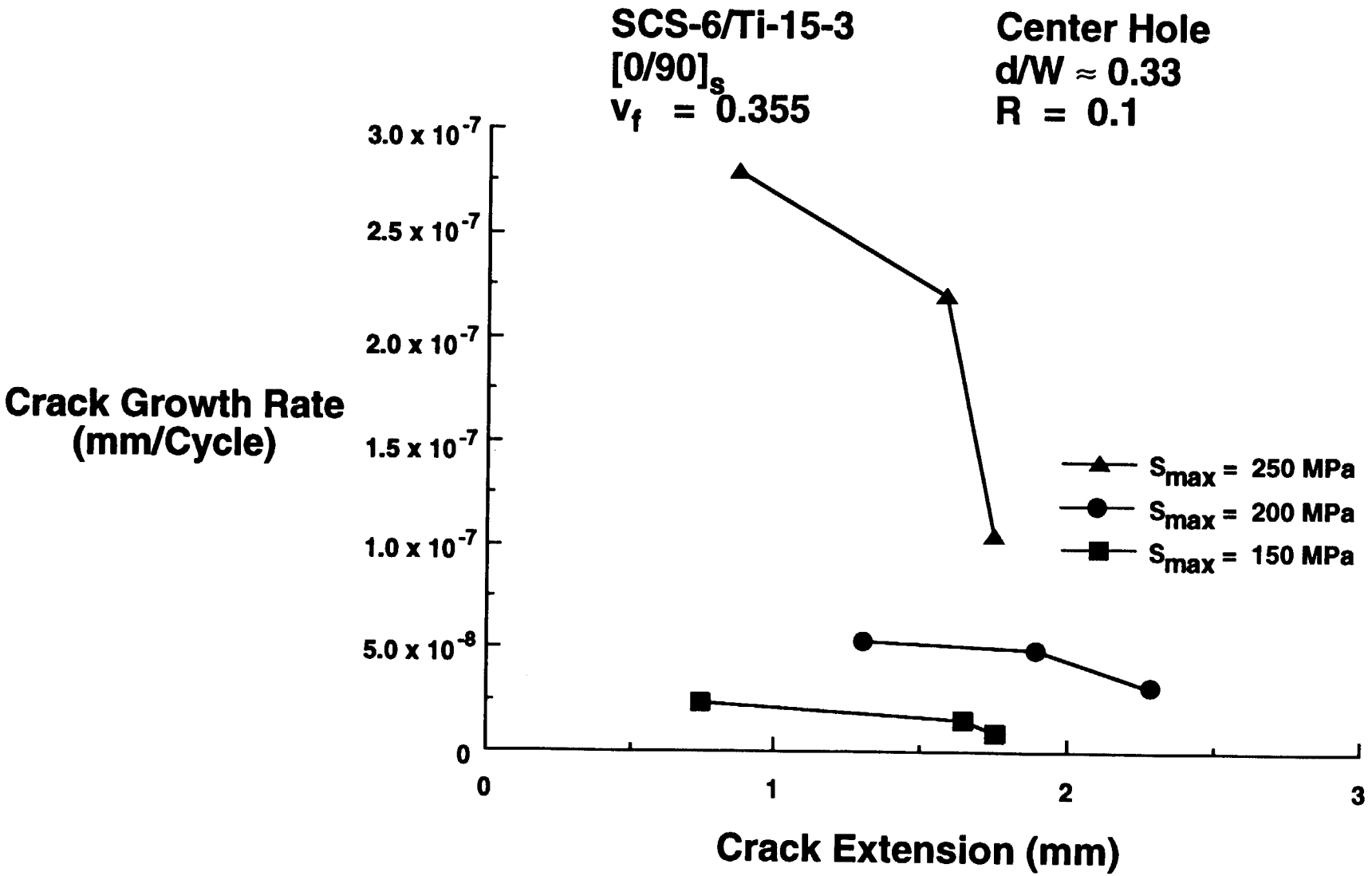

Figure 8. Crack growth rate as a function of number of cycles in cross ply, SCS-6/Ti-15-3 laminates containing holes.

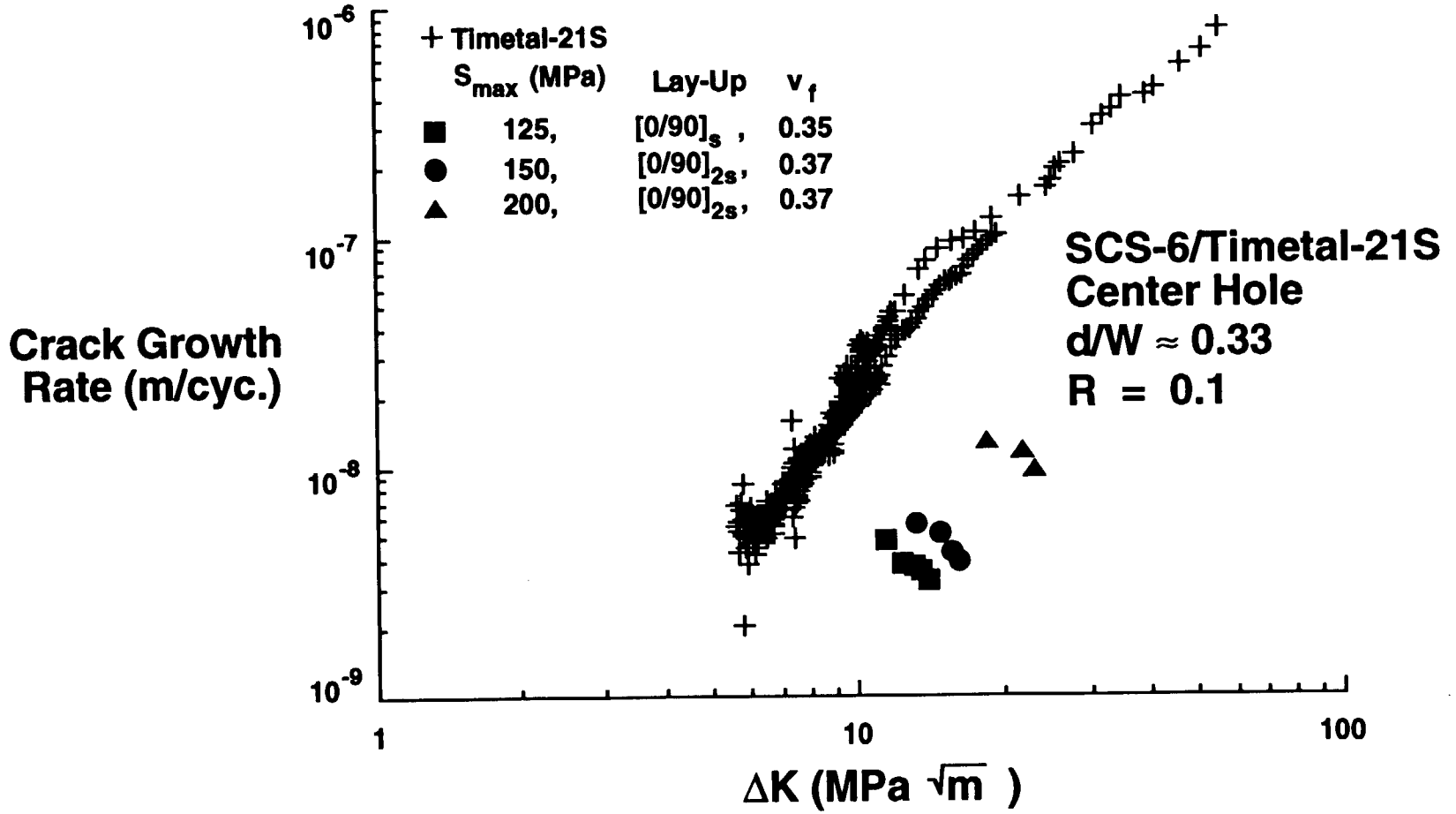

Figure 9. Crack growth rate as a function of the applied stress intensity factor range for given values of applied stress in cross ply, SCS-6/Timetal-21S laminates containing holes.

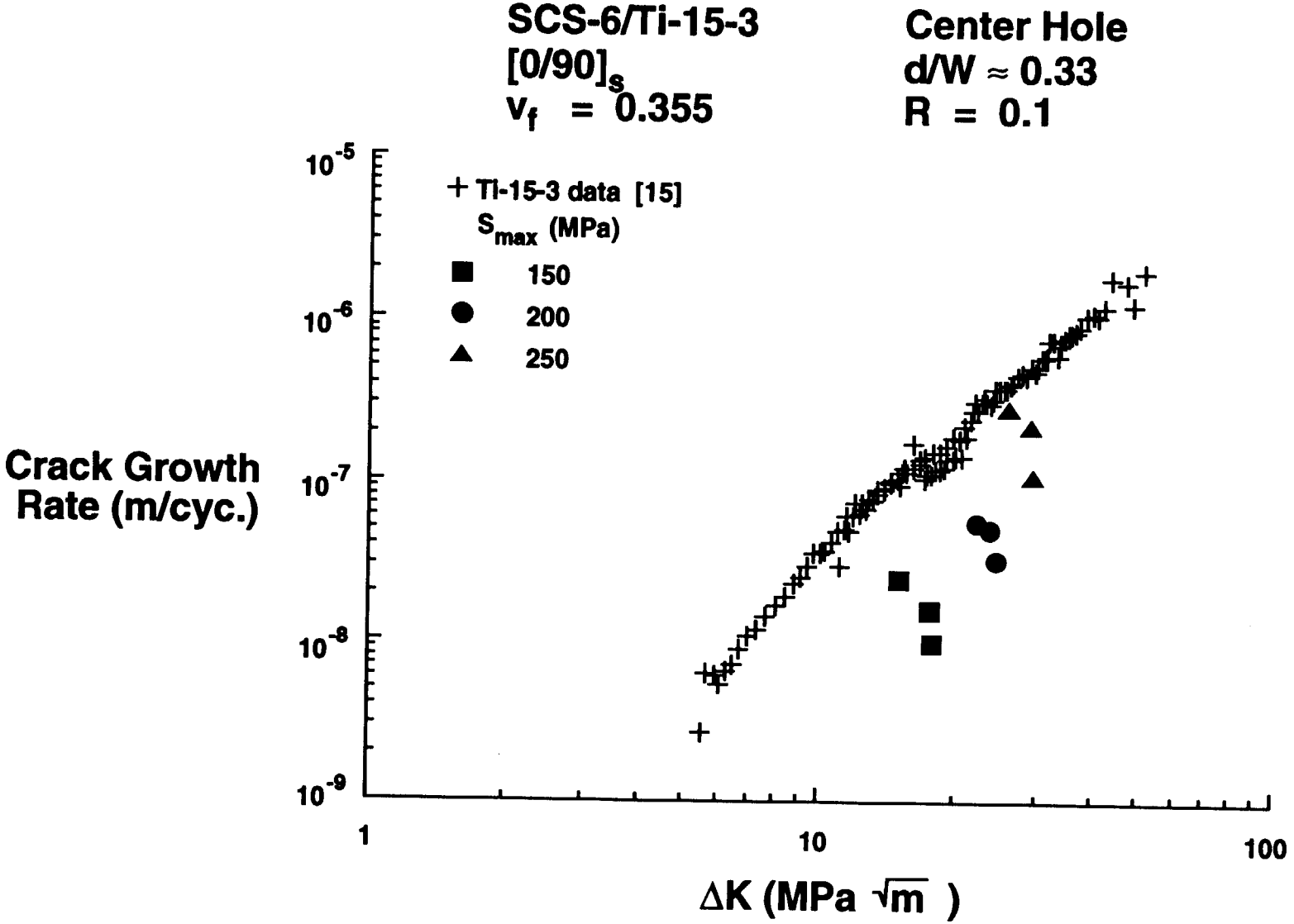

Figure 10. Crack growth rate as a function of the applied stress intensity factor range for given values of applied stress in cross ply, SCS-6/Ti-15-3 laminates containing holes.

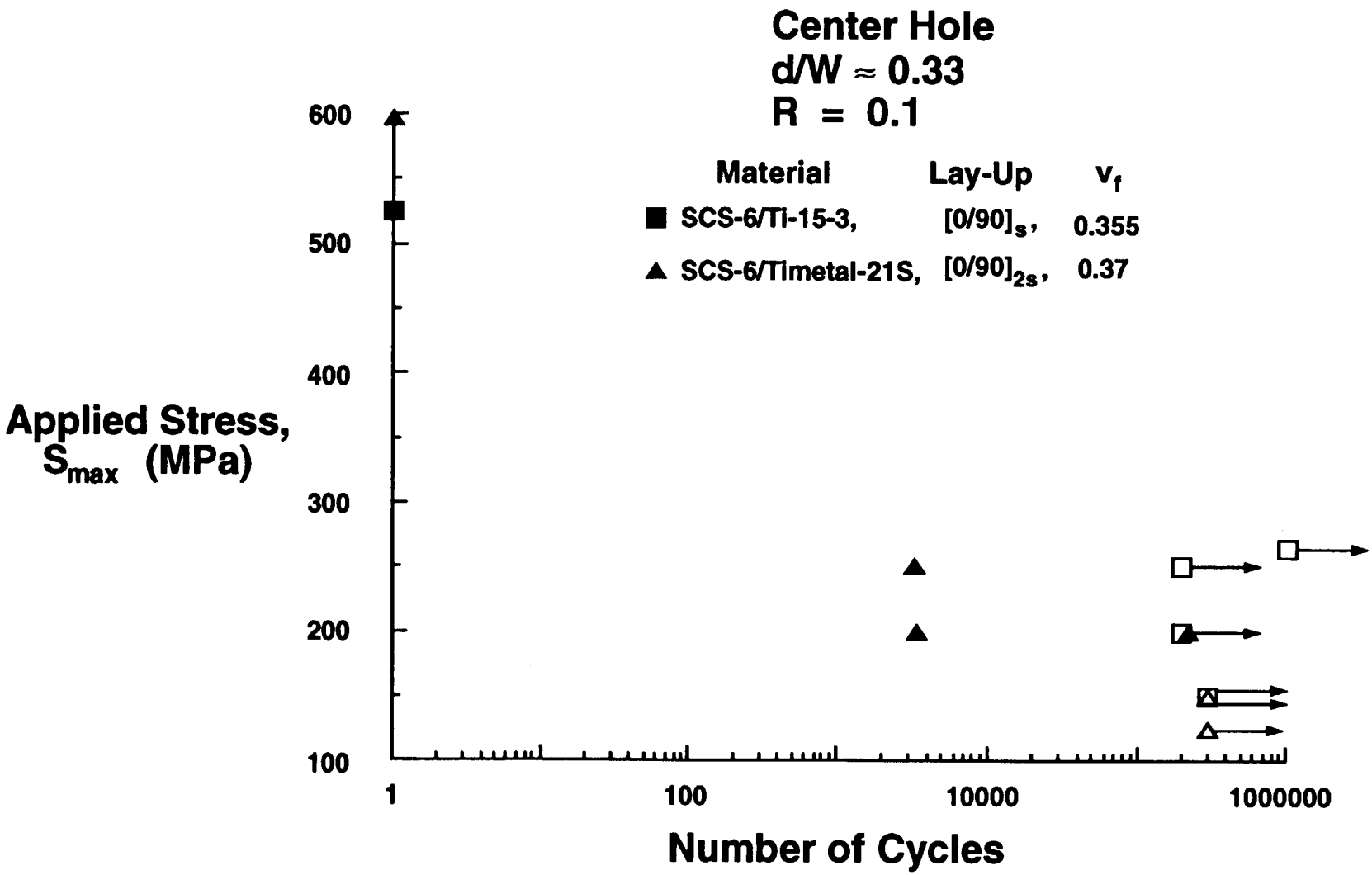

Figure 11. Applied stress as a function of number of cycles to failure (solid symbols) and applied stress as a function of cycles to test termination (open symbols) for cross ply titanium matrix composites containing center holes.

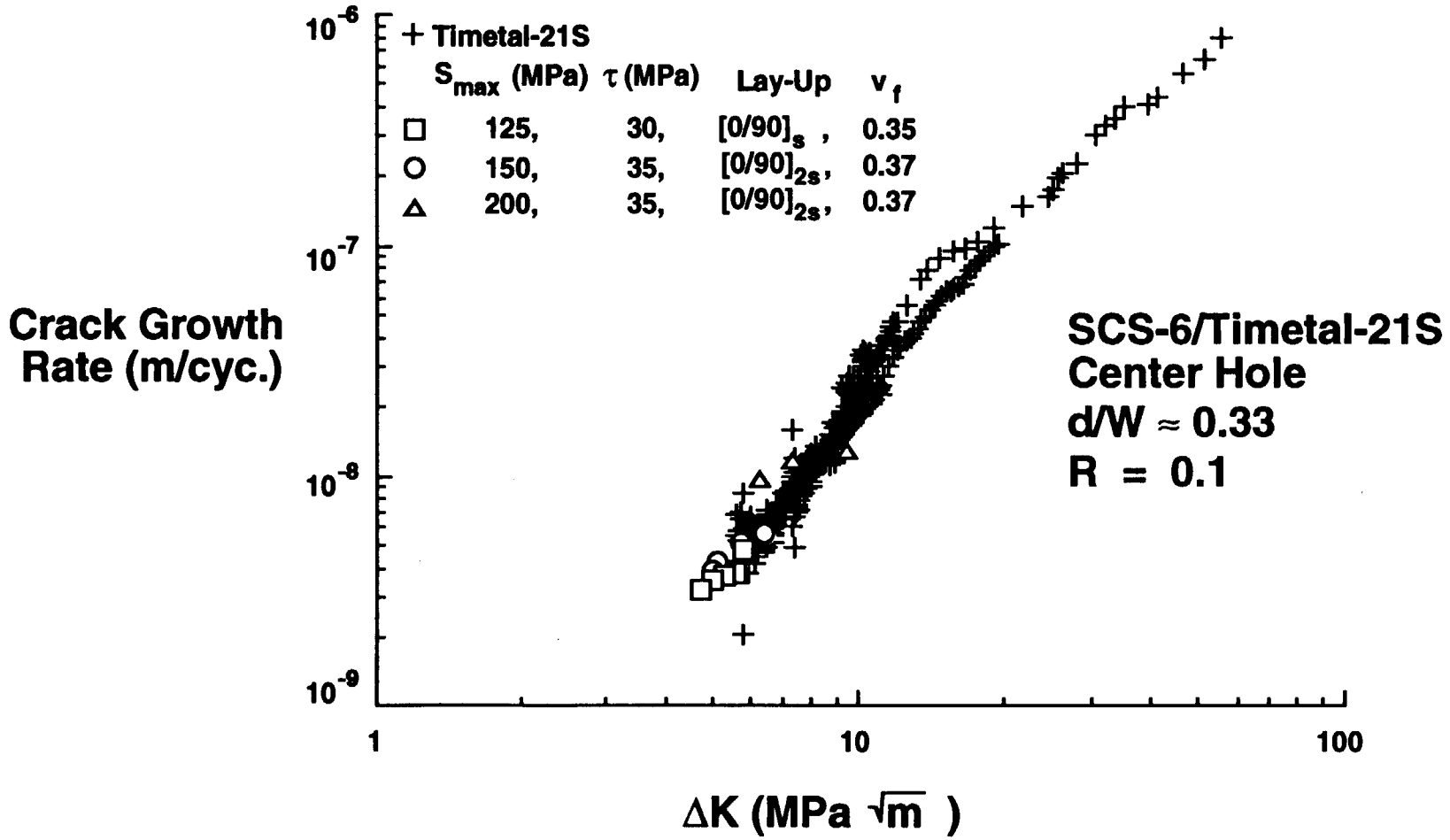

Figure 12. Crack growth rate as a function of stress intensity factor range for given values of applied stress in cross ply, SCS-6/Timetal-21S laminates containing holes.

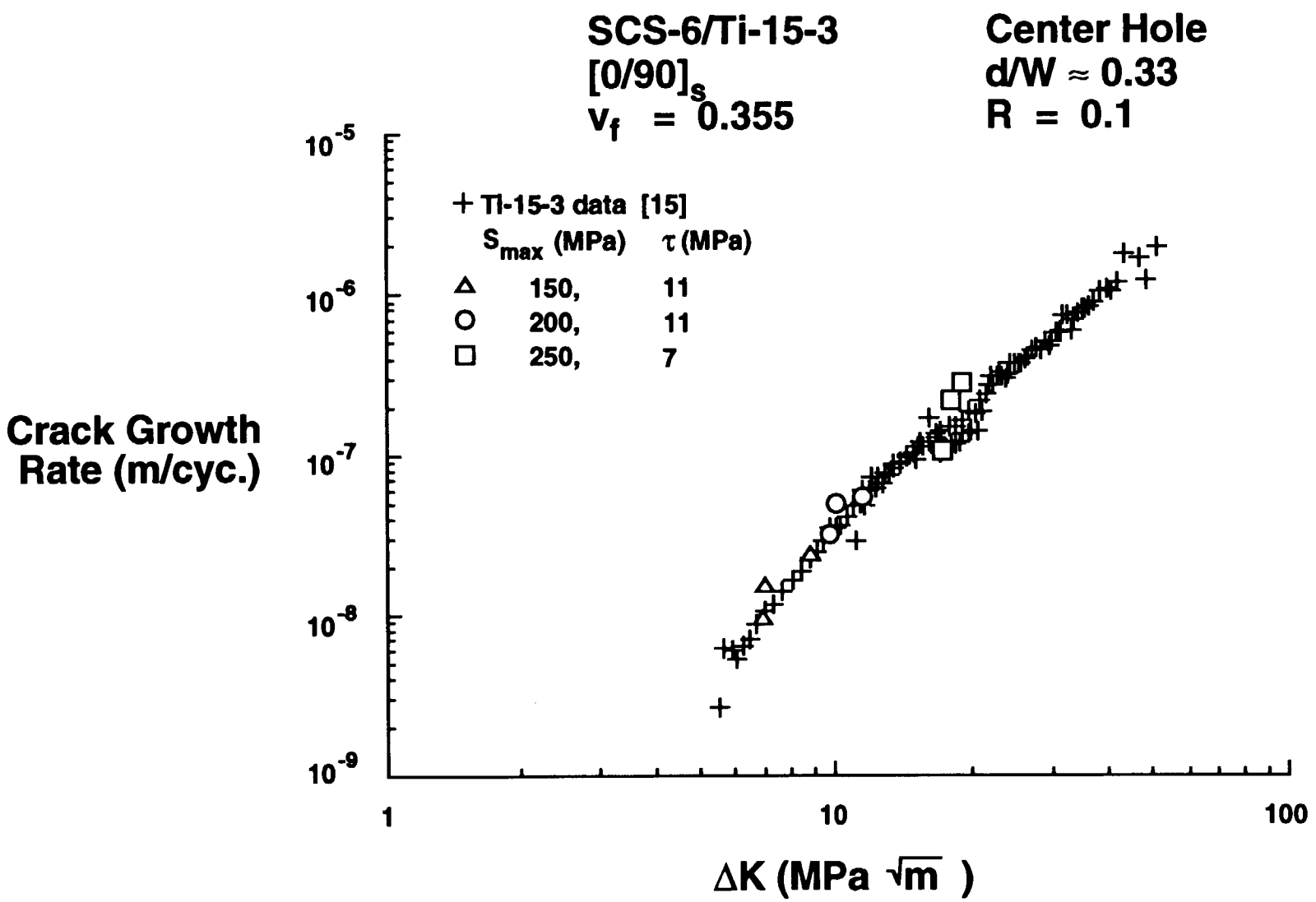

Figure 13. Crack growth rate as a function of stress intensity factor range for given values of applied stress in cross ply, SCS-6/Ti-15-3 laminates containing holes.

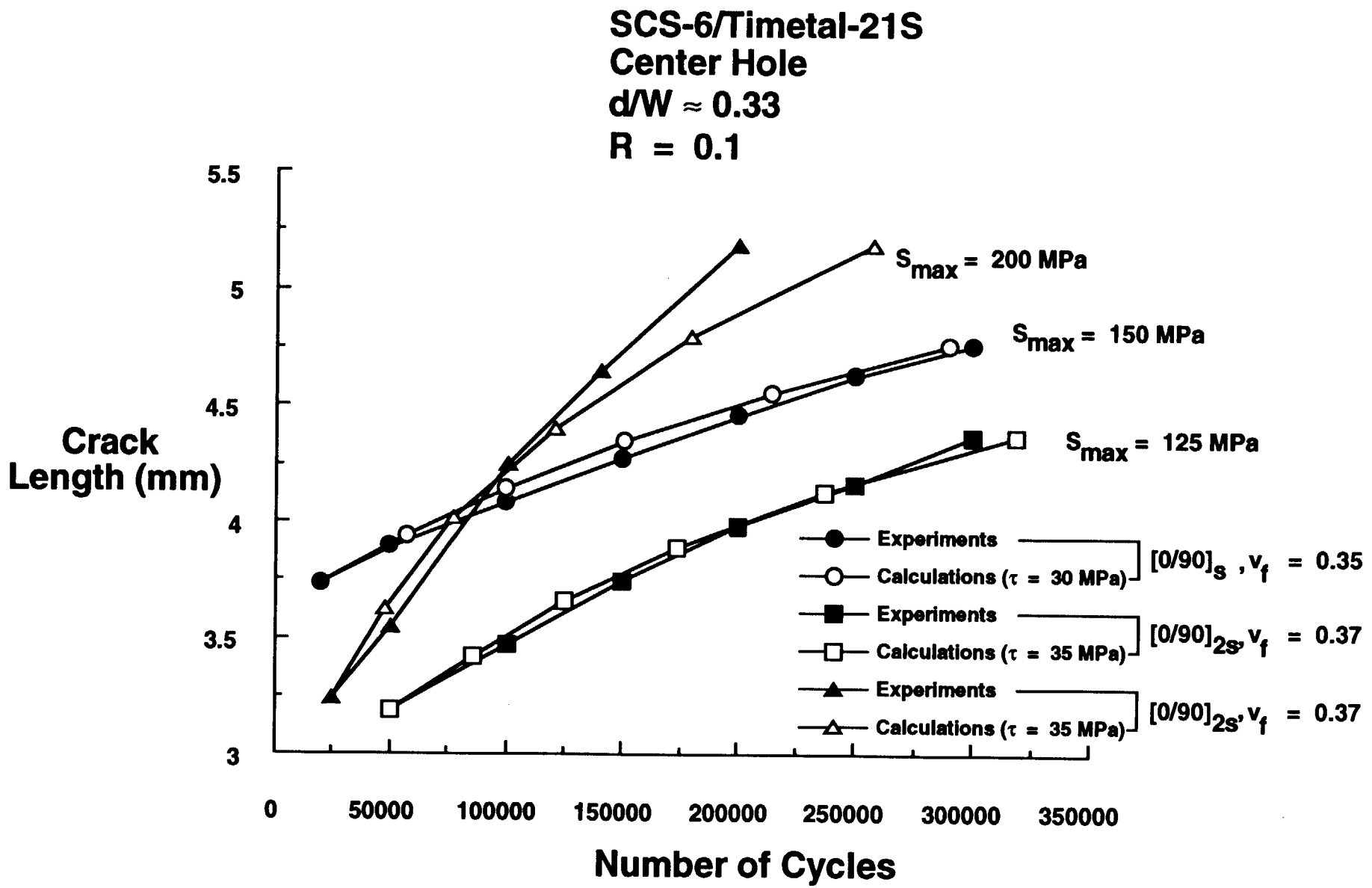

Figure 14. Measured and calculated average crack length as a function of number of cycles in cross ply, SCS-6/Timetal-21S laminates containing holes.

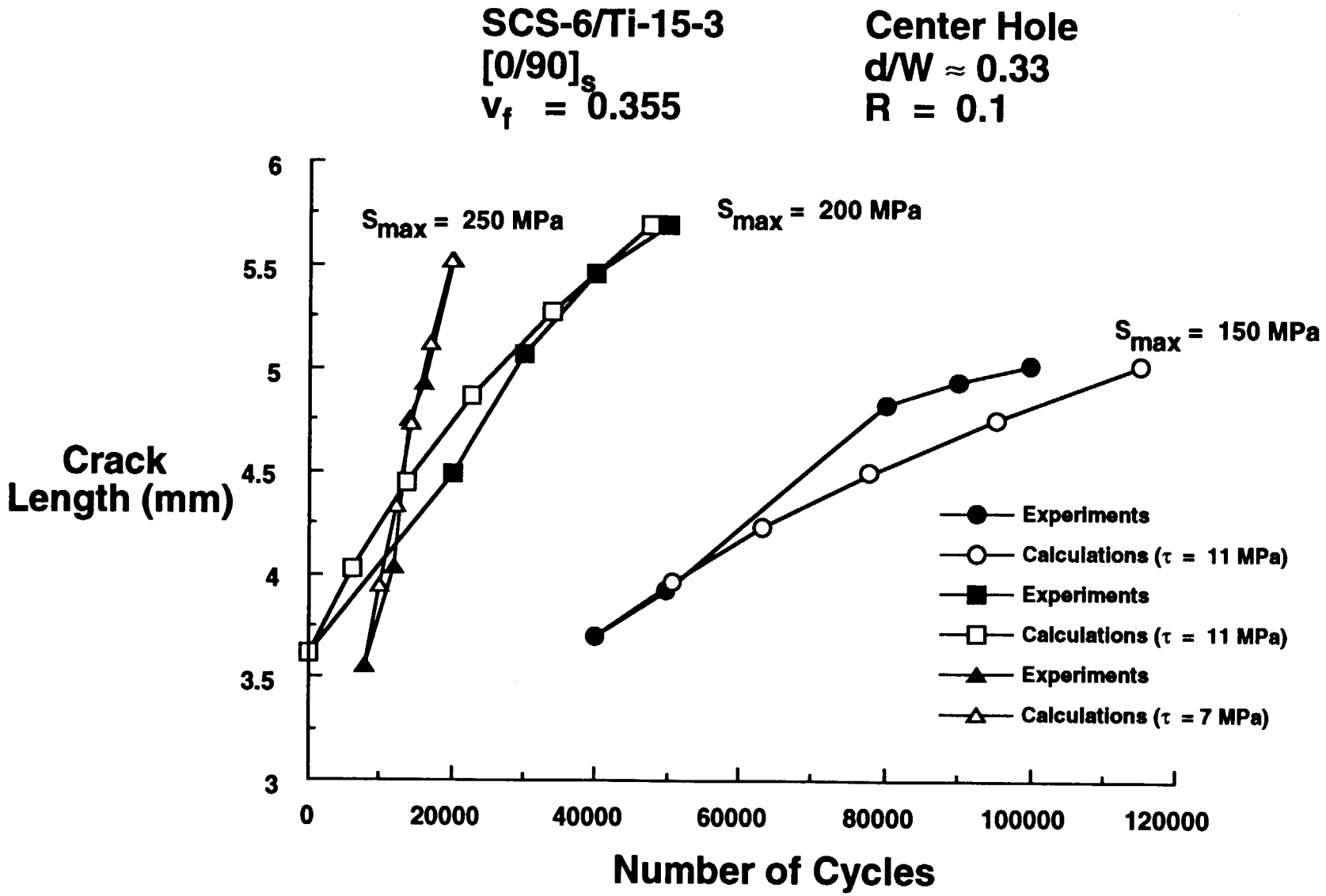

Figure 15. Measured and calculated average crack length as a function of number of cycles in cross ply, SCS-6/Ti-15-3 laminates containing holes.

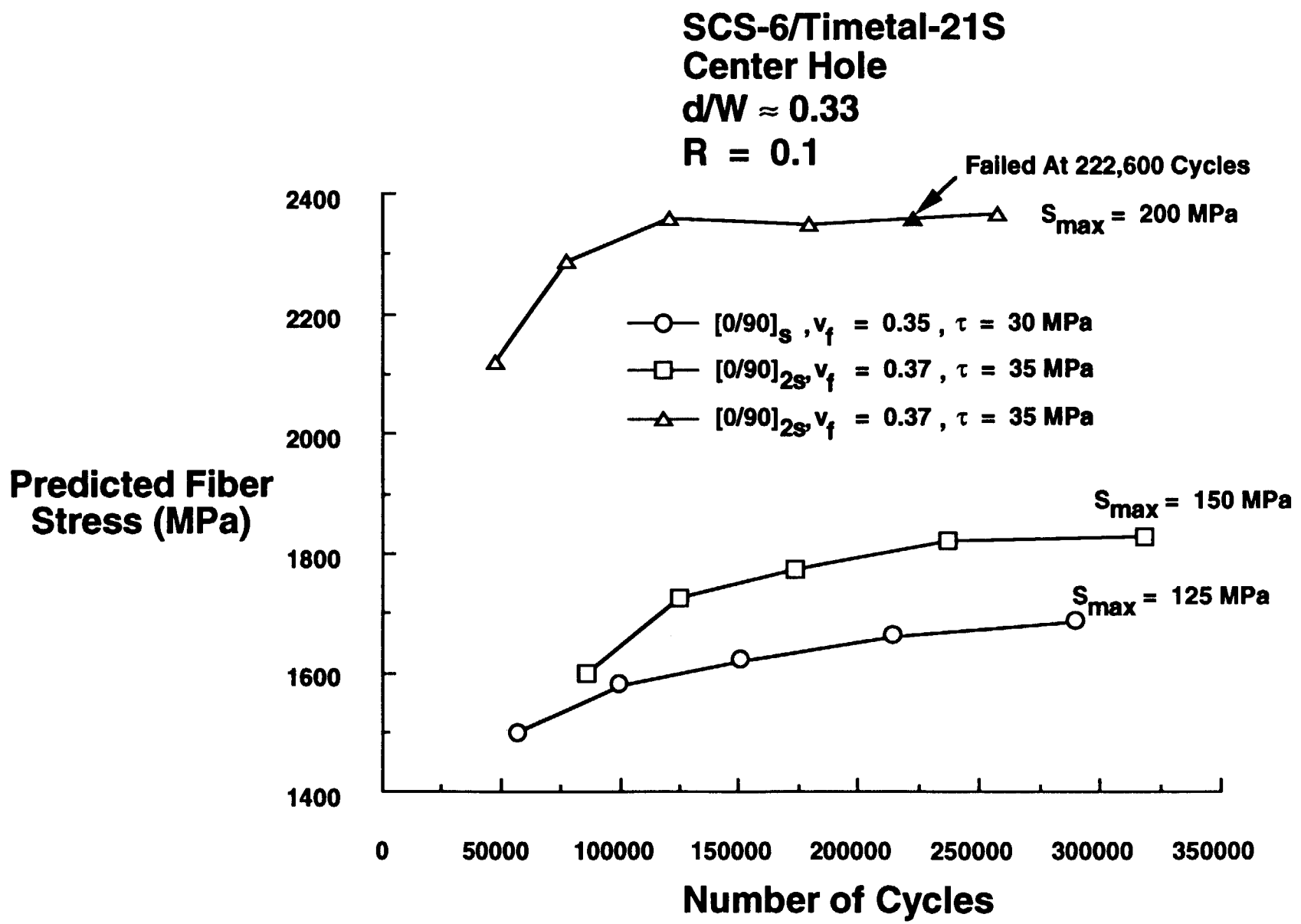

Figure 16. Stress in first intact fiber as a function of number of cycles in cross ply, SCS-6/Timetal-21S laminates containing holes.

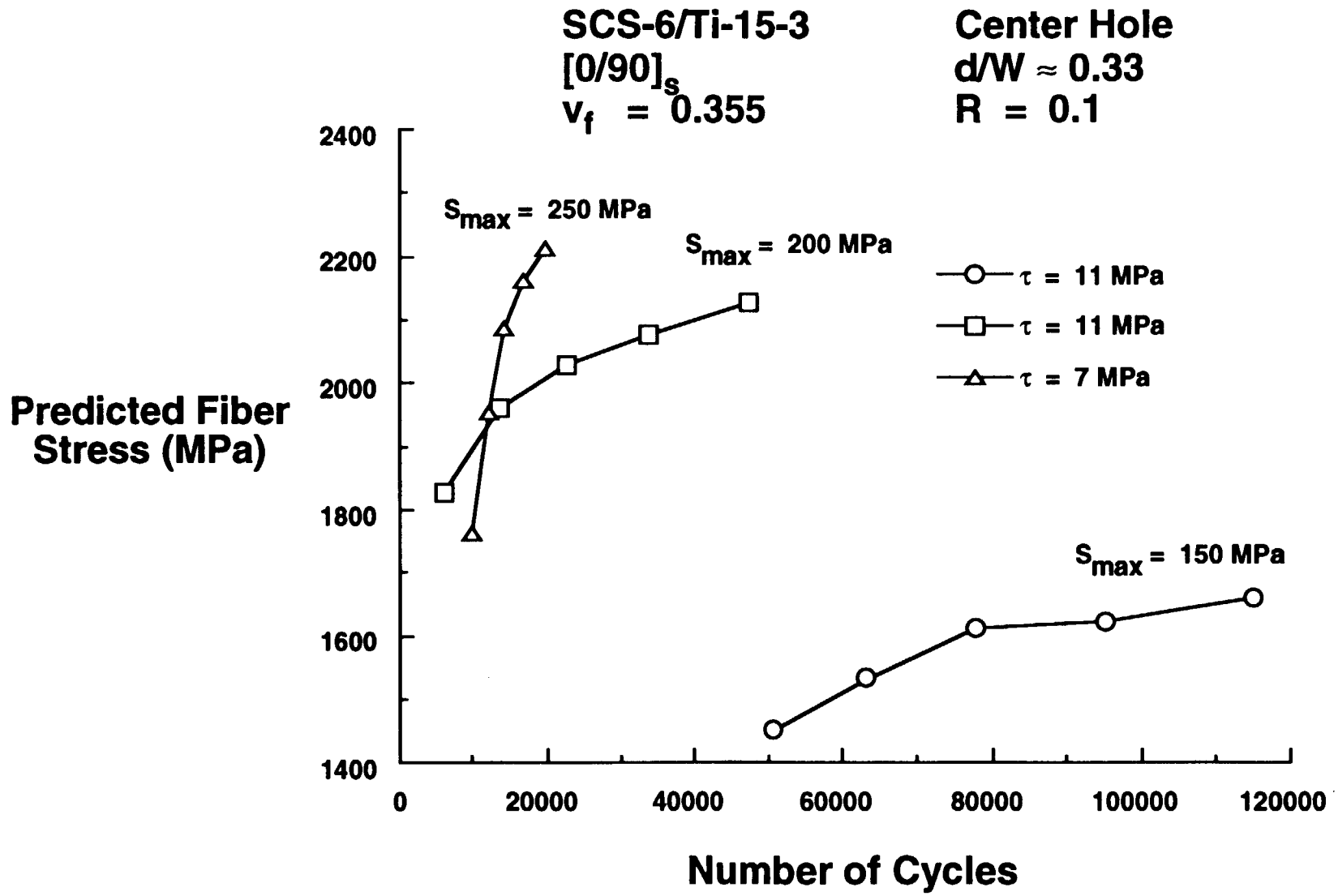

Figure 17. Stress in first intact fiber as a function of number of cycles in cross ply, SCS-6/Ti-15-3 laminates containing holes.

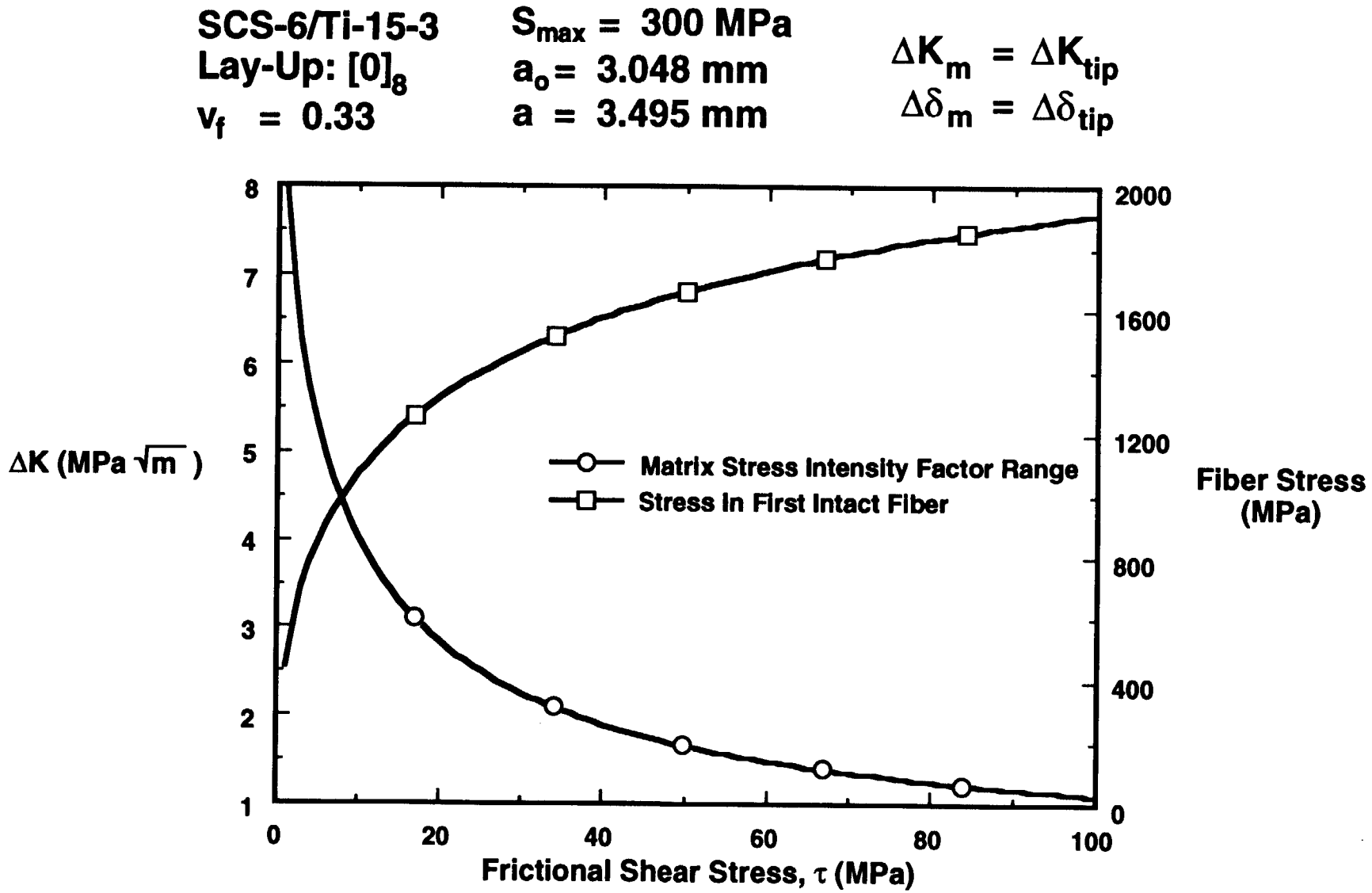

Figure 18. Stress intensity factor range in matrix and stress in first intact fiber as a function of the interfacial frictional shear. As τ increases, the stress in the first intact fiber increases, thus, promoting fiber breakage. As τ decreases, the matrix stress intensity factor range increases, thus, promoting matrix cracking [6].

REPORT DOCUMENTATION PAGE

Form Approved
OMB No. 0704-0188

1. AGENCY USE ONLY (Leave blank)	2. REPORT DATE	3. REPORT TYPE AND DATES COVERED
	May 1993	Technical Memorandum

4. TITLE AND SUBTITLE
Modeling Fatigue Crack Growth in Cross Ply Titanium Matrix Composites

5. FUNDING NUMBERS
763-23-45-85

6. AUTHOR(S)
J. G. Bakuckas, Jr. and W. S. Johnson

7. PERFORMING ORGANIZATION NAME(S) AND ADDRESS(ES)
NASA Langley Research Center
Hampton, VA 23681-0001

8. PERFORMING ORGANIZATION REPORT NUMBER

9. SPONSORING / MONITORING AGENCY NAME(S) AND ADDRESS(ES)
National Aeronautics and Space Adminstration
Washington, DC 20546-0001

10. SPONSORING / MONITORING AGENCY REPORT NUMBER
NASA TM-108988

11. SUPPLEMENTARY NOTES
Bakuckas, Jr.: NRC, Langley Research Center, Hampton, VA; Johnson: MEMB, Langley Research Center, Hampton, VA. Presented to ASTM for Fifth Symposium on Composite Materials: Fatigue and Fracture; Atlanta, GA; May 4-6, 1993.

12a. DISTRIBUTION / AVAILABILITY STATEMENT
Unclassified-Unlimited

Subject Category 24

12b. DISTRIBUTION CODE

13. ABSTRACT *(Maximum 200 words)*

In this study, the fatigue crack growth behavior of fiber bridging matrix cracks in cross-ply SCS-6/Ti-15-3 and SCS-6/Timetal-21S laminates containing center holes was investigated. Experimental observations revealed that matrix cracking was far more extensive and wide spread in the SCS-6/Ti-15-3 laminates compared to that in the SCS-6/Timetal-21S laminates. In addition, the fatigue life of the SCS-6/Ti-15-3 laminates was significantly longer than that of the SCS-6/Timetal-21S laminates. The matrix cracking observed in both material systems was analyzed using a fiber bridging (FB) model which was formulated using the boundary correction factors and weight functions for center hole specimen configurations. A frictional shear stress is assumed in the FB model and was used as a curve fitting parameter to model matrix crack growth data. The higher frictional shear stresses calculated in the SCS-6/Timetal-21S laminates resulted in lower stress intensity factors in the matrix and higher axial stresses in the fibers compared to those in the SCS-6/Ti-15-3 laminates at the same applied stress levels.

14. SUBJECT TERMS
Fiber bridging; Matrix cracking; Fiber-matrix debonding; Stress intensity factor range; Crack growth behavior

15. NUMBER OF PAGES
35

16. PRICE CODE
A03

17. SECURITY CLASSIFICATION OF REPORT	18. SECURITY CLASSIFICATION OF THIS PAGE	19. SECURITY CLASSIFICATION OF ABSTRACT	20. LIMITATION OF ABSTRACT
Unclassified	Unclassified		